Available online at www.sciencedirect.com
SCIENCE DIRECT®
Journal of Magnetic Resonance 161 (2003) 234–241
JMR Journal of Magnetic Resonance
www.elsevier.com/locate/jmr

Interference of homonuclear decoupling and exchange in the solid-state NMR of perfluorocyclohexane

Deborah E. McMillan,[a] Paul Hazendonk,[b] and Paul Hodgkinson[a,*]

[a] *Department of Chemistry, University of Durham, Stockton Road, Durham DH1 3LE, UK*
[b] *Department of Chemistry and Biochemistry, University of Lethbridge, 4401 University Drive, Lethbridge, Alta., Canada T1K 3M4*

Received 3 October 2002; revised 10 January 2003

Abstract

We observe an interference between RF irradiation used for homonuclear decoupling of ^{19}F and conformational exchange in the ^{13}C spectrum of perfluorocyclohexane. We show that these effects can be readily reproduced in simulation, and characterise their dependence on the various NMR and experimental parameters. Their application to observing exchange rates on the kHz timescale is evaluated with respect to $T_{1\rho}$ measurements and the connections between the two approaches established. The implications for experiments that use homonuclear decoupling of ^{1}H to resolve $^{1}J_{CH}$ couplings in the solid-state are also evaluated in detail.

Keywords: Solid-state; NMR; Exchange; Decoupling; J-coupling; F-19

1. Introduction

In the solution-state NMR of organic molecules, *J*-couplings provide invaluable information about chemical bonding. In contrast, the observation of *J*-couplings in the solid-state NMR of these systems is hampered by the presence of much stronger dipolar couplings, which cannot be sufficiently suppressed by magic-angle spinning. Current probe designs permit the application of radio-frequency fields for homonuclear decoupling that are sufficiently strong (say 150 kHz) that proton linewidths can be reduced to the point where one-bond $^{1}J_{CH}$ couplings can be resolved. As a result, a wide variety of *J*-coupling-based experiments can be adapted to solid samples [1–3].

Such methods should work equally well with fluorinated organics, although the much larger chemical shift range of ^{19}F compared to ^{1}H may challenge current homonuclear decoupling methods. Perfluorocyclohexane, C_6F_{12}, would appear to be a suitable test sample; it is a plastic crystal and so the strong intramolecular couplings are suppressed by the rapid (and isotropic) motion of the molecules. Unfortunately, as Fig. 1 shows, the $^{1}J_{CF}$ couplings are not resolved at room temperature. The (scaled) 1:2:1 triplet expected from the CF_2 groupings of C_6F_{12} under ^{19}F homonuclear decoupling, only appears clearly when the temperature is lowered below −30 °C. We decided to investigate this behaviour, as it is likely to be relevant to the more general application of "*J*-coupling experiments" to the solid-state.

From previous solution-state [4], liquid-state [5], and solid-state experiments [6], we know that perfluorocyclohexane undergoes chair–chair conformational exchange, in addition to its isotropic re-orientation. From the data derived from *solution-state* experiments [4] (as revised in [7]), we estimate the rate of exchange at 25 °C to be 32 kHz. This is of the same order of magnitude as the radio-frequency "field strength" expressed in frequency units (about 50 kHz). In contrast, the exchange is predicted to be of the order of Hz at −50 °C. It is thus reasonable to suppose that an interference between the conformational exchange and spin dynamics due to the RF irradiation is causing the collapse of the triplet structure in the ambient temperature experiment.

Interference between continuous-wave *heteronuclear* decoupling and exchange have previously been observed and characterised in solids [8]. Loss of resolution caused

* Corresponding author. Fax: +44-191-384-4737.
E-mail address: paul.hodgkinson@durham.ac.uk (P. Hodgkinson).

1090-7807/03/$ - see front matter © 2003 Elsevier Science (USA). All rights reserved.
doi:10.1016/S1090-7807(03)00015-6

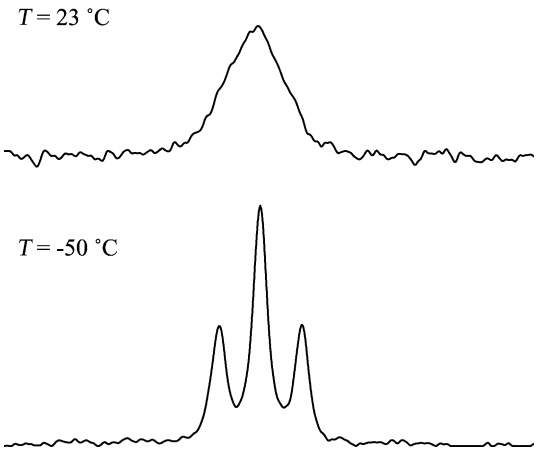

Fig. 1. ^{13}C NMR spectra of perfluorocyclohexane (C_6F_{12}) acquired during BLEW-12 homonuclear decoupling of the ^{19}F ($\nu_{rf} = 83$ kHz) at two different temperatures.

by interference between *homonuclear* decoupling and exchange has also been observed in CRAMPS-style spectra, i.e., where the abundant spin spectrum is observed during homonuclear decoupling [6,9,10]. The indirect effect of homonuclear decoupling on the X-nucleus spectrum and its impact on coherence transfers using J-couplings has not, to our knowledge, been characterised in any detail. In this paper, we consider the interplay between exchange and homonuclear decoupling, and show that the behaviour in C_6F_{12} system can be readily reproduced, and, in simple cases, connected to earlier semi-classical approaches. The final sections discuss the application of these effects to the measurement of exchange rates and their impact on experiments that rely on the resolution of J-couplings in the solid-state.

2. Characterisation

Because C_6F_{12} is a plastic crystal, *intra*molecular dipolar interactions and chemical shift anisotropies are eliminated by the isotropic motion. *Inter*molecular dipolar interactions are not removed by the motion, but are relatively small and can be assumed to be eliminated by the homonuclear decoupling. Given that only one-bond J-couplings are significant—$^2J_{CF}$ are typically an order of magnitude smaller than $^1J_{CF}$ [11]—we can hope to model the system in terms of the behaviour of a single CF_2 system. The rotating-frame Hamiltonian (in frequency units) is thus

$$H(t) = J_{eq} I_{1z} S_z + J_{ax} I_{2z} S_z + \delta_{eq} I_{1z} + \delta_{ax} I_{2z} + H_{rf}(t), \qquad (1)$$

where J_{eq} and J_{ax} are the $^1J_{CF}$ couplings with equatorial and axial fluorines, respectively, and δ_{eq} and δ_{ax} are the ^{19}F chemical shifts (the ^{13}C chemical shift simply determines the position of the peak in the ^{13}C spectra and has no effect on the spin dynamics).

The Hamiltonian for the RF involves (phase-modulated) irradiation of the I spins only:

$$H_{rf}(t) = \nu_{rf}(\cos\phi(t) F_x + \sin\phi(t) F_y), \qquad (2)$$

where $F_x = I_{1x} + I_{2x}$, etc. are sum operators, ν_{rf} is the RF amplitude, and $\phi(t)$ is the time-dependent RF phase.

We can slightly simplify Eq. (1) by writing $J = J_{eq} = J_{ax}$ (any differences between the couplings to axial and equatorial sites are too small to be resolved) and assuming that the ^{19}F transmitter is centred in the ^{19}F spectrum, i.e., the ^{19}F shifts can parameterised simply in terms of the difference in chemical shift, Δ. The simplified Hamiltonian is thus

$$H(t) = J F_z S_z + (\Delta/2) I_{1z} - (\Delta/2) I_{2z} + \nu_{rf}(\cos\phi(t) F_x + \sin\phi(t) F_y). \qquad (3)$$

The Hamiltonian is block diagonal since m_z of the S spin is a good quantum number.

The conformational exchange has the effect of (instantaneously) interconverting equatorial and axial sites. The simplest approach to including this exchange is to formulate the problem in Liouville space. The Liouvillian is thus

$$\hat{L} = -2\pi i \hat{H} + k(\hat{X} - \mathbf{1}), \qquad (4)$$

where $\hat{H} = [[H,],]$ is the double commutator ($H \otimes \mathbf{1} - \mathbf{1} \otimes H^T$, where $\mathbf{1}$ is an identity matrix of the same order as the Hilbert space). k is the rate of equatorial–axial exchange, and $\hat{X}$ is the exchange matrix linking Liouville states that are interconverted by the exchange. The single caret used to distinguish operators/matrices in Liouville space can be dropped as the following description is entirely within Liouville space. Since the exchange only "mixes" the I spins, the Liouvillian also has a block structure, consisting of four 16×16 blocks. Taking advantage of this block structure would improve the efficiency of the calculation (in practice, the calculations were sufficiently rapid using the full 64×64 Liouville space).

The Liouville space propagator over a time interval Δt is simply $U = \exp(L\Delta t)$. For BLEW-12 [12] and related sequences where the phases are all multiples of 90 °, it is convenient to calculate the four propagators, U_x, U_{-x}, U_y, U_{-y}. The propagator over a BLEW-12 cycle (duration τ_c) is then efficiently determined by

$$U(\tau_c, 0) = U_{-x} U_{-y} U_x U_{-y} U_{-x} U_{-y} U_y U_x U_y U_{-x} U_y U_x. \qquad (5)$$

For time-dependent decoupling sequences, it is convenient to use τ_c as the dwell time for sampling of the evolution, since the signal is then determined by this single propagator, $U(\tau_c, 0)$. Note that the presence of exchange means that we must include the time-dependence of the pulse sequence explicitly rather than using the usual average Hamiltonian for the BLEW sequence.

With an initial density matrix $\sigma(0) = S_x$, the NMR signal on the S spin is then

$$S(n\tau_c) = \mathrm{tr}(S_+ U(\tau_c, 0)^n S_x). \quad (6)$$

The calculation of the signal can be made more efficient by transformation into the eigenbasis of U [13,14].

3. Experimental

A 7.5 mm Chemagnetics PENCIL rotor was filled with perfluorocyclohexane (Aldrich) and the rotor "sealed" using a Vespel cap. First attempts to acquire spectra with unsealed rotors failed since the C_6F_{12} quickly sublimes under the conditions used (fast gas flows required for the variable temperature control). The spectra were acquired on a Chemagnetics CMXII spectrometer with a nominal proton frequency of 200 MHz. The ^{19}F transmitter was placed in the centre of ^{19}F spectrum to minimise off-resonance effects on the homonuclear decoupling.

^{13}C spectra were acquired as a function of temperature using direct excitation of the ^{13}C magnetisation under BLEW-12 ^{19}F homonuclear decoupling. Only modest spin rates were used to improve B_0 inhomogeneity, and so frictional heating is assumed to be negligible. Fig. 2 shows a comparison between the experimental spectra and spectra simulated using the model described above. The simulated spectra and corresponding exchange rate were obtained by iterative fitting of the experimental spectra, using the procedure outlined below.

In general, the correlation between linewidth and exchange is too strong to permit both the rate and linewidth to be fitted simultaneously. Hence the exchange-free linewidth was measured from the lowest temperature spectrum (the rate of exchange here is negligible in comparison to v_{rf}). This was assumed to be the same in all spectra. It was not possible to measure the exchange-free linewidth in the $k \gg v_{rf}$ limit, which would otherwise have provided a check on the validity of this assumption.

The spectra are quite sensitive to the exact value of v_{rf} since the scaling factor of the decoupling sequence is very sensitive to experimental variations. Although the probe was retuned at each temperature and the effective 90° length did not measurably drift over the course of the experiment, satisfactory fits were only possible by making v_{rf} a fitted parameter. The strong correlation of the actual v_{rf} (and hence scaling factor) with J again means these parameters cannot be fitted independently. The estimated value of 250 Hz for $^1J_{CF}$ was confirmed from the ^{13}C spectrum of C_6F_{12} in d_{10}-toluene (the $^1J_{CF}$ sufficiently dominates longer range couplings to allow it to be estimated to within 10 Hz).

The difficulties of precisely measuring correlated parameters such as $^1J_{CF}$, v_{rf} and exchange-free linewidth mean that the rates obtained should be treated with some caution. In addition, the spectra above

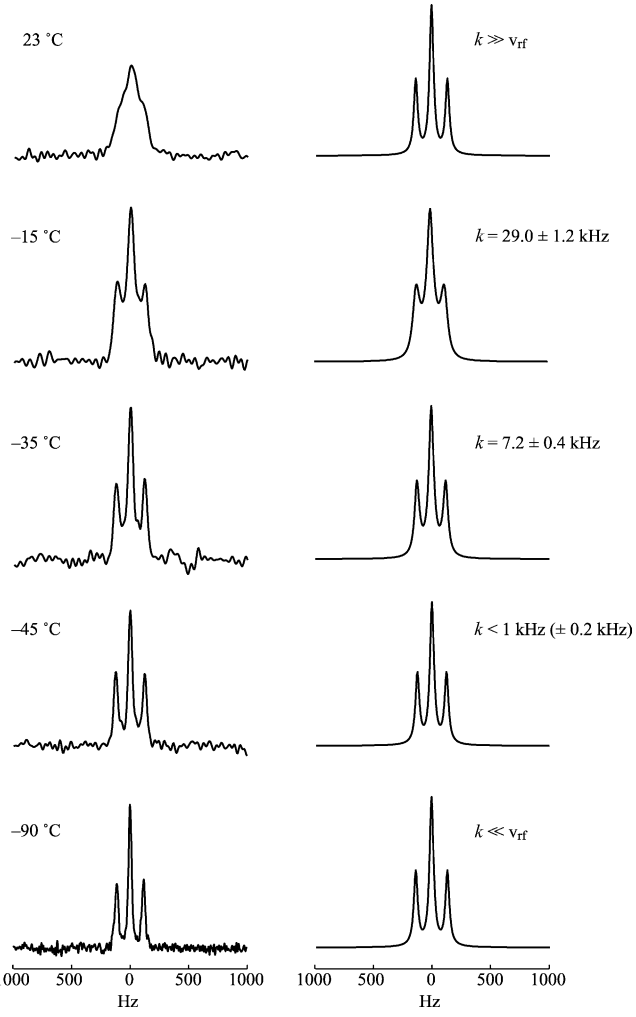

Fig. 2. Left: ^{13}C NMR spectra of C_6F_{12} using BLEW-12 decoupling, as a function of temperature ($v_{rf} = 50$ kHz). Right: fitted spectra (except spectra for $T = -90$ °C and $T = 23$ °C which are calculated using $k = 0$ and $k = 10^6$ Hz, respectively, where k is the rate of conformational exchange).

$T > -10$ °C could not be fitted as the signal collapses into a broad unresolved feature rather than sharpening once more into a 1:2:1 triplet in the limit $k \gg v_{rf}$. As confirmed by ^{19}F $T_{1\rho}$ measurements (shown later), additional relaxation mechanisms come into play at the sample approaches its sublimation point (presumably from additional motional processes, such as translational diffusion). With $T_{1\rho}$ remaining short, the $^1J_{CF}$ remains unresolved.

4. Application to rate measurement

Although this interference between decoupling and exchange is a potential problem for experiments relying on resolved J-couplings, it does provide a potential means of measuring exchange rates that are on the same timescale as the RF irradiation, i.e., 10's of kHz. In this

section, we discuss the advantages and drawbacks of this approach compared to alternative methods.

Other methods to probe exchange on this timescale also exploit interference between RF irradiation and the exchange. In each case, we expect the interference to be proportional to $J(\omega_{\text{eff}})$, the spectral density of the motion at an "effective" RF irradiation frequency:

$$\frac{1}{T_c} \propto \frac{\tau}{1+\tau^2\omega_{\text{eff}}^2}, \tag{7}$$

where $\tau = 1/2k$ is the correlation time for the two-site exchange at a given temperature, and T_c is a time constant. This time constant is a T_2 (or rather the contribution of exchange to the effective T_2) in the case of interference with *heteronuclear* (CW) decoupling, i.e., observing the S spin during CW irradiation of the I spins [8,16]. Alternatively, T can be a $T_{1\rho}$ for relaxation under a spin-lock. The nature of the proportionality depends on the model for the relaxation, but is not important when obtaining activation barriers for the motion, since only the logarithm of $1/T_c$ as function of inverse temperature is required.

The effect of two-site exchange on $T_{1\rho}$ during off-resonance (CW) decoupling has been previously characterised using a semi-classical approach [17]:

$$\frac{1}{T_{1\rho}} = \frac{\sin^2\theta\Delta^2}{4}\frac{\tau}{1+4\pi^2\tau^2v_{\text{eff}}^2}, \tag{8}$$

where θ is the tilt angle of the effective field with ($v_{\text{eff}} = v_{\text{rf}}/\sin\theta$). The maximum interference (corresponding to a minimum in the value of $T_{1\rho}$) occurs when $4\pi^2\tau^2v_{\text{eff}}^2 = 1$. In the case of Lee–Goldburg decoupling ($\theta = 54.7°$), this corresponds to $k = \pi v_{\text{rf}}\sqrt{3/2}$. We show in the appendix how Eq. (8) can be derived in the context of the Liouville space propagation described in the previous section. Note that measuring $T_{1\rho}$ under Lee–Goldburg conditions has the advantage of suppressing "spin diffusion," helping to localise the effects of the motion to the molecular fragment involved.

The observation of exchange via *homonuclear* decoupling has essentially the same characteristics. In the intermediate regime, $v_{\text{rf}} \sim k$, the spectra can be fitted to obtain exchange rates, although, as described above, the strong correlation between different parameters means that obtaining absolute rates is a delicate business. The only advantage of this approach that may justify its increased complexity is that the entire spectrum is used to extract rate parameters. As demonstrated by the widespread use of ^{2}H NMR spectra in studies of molecular dynamics, an exact fit of a non-trivial spectrum permits a clear justification of the motional model.

Fig. 3 plots a set of $T_{1\rho}$ values measured for C_6F_{12} as a function of temperature in a form appropriate to fitting to the Eyring equation for the temperature dependence of rates:

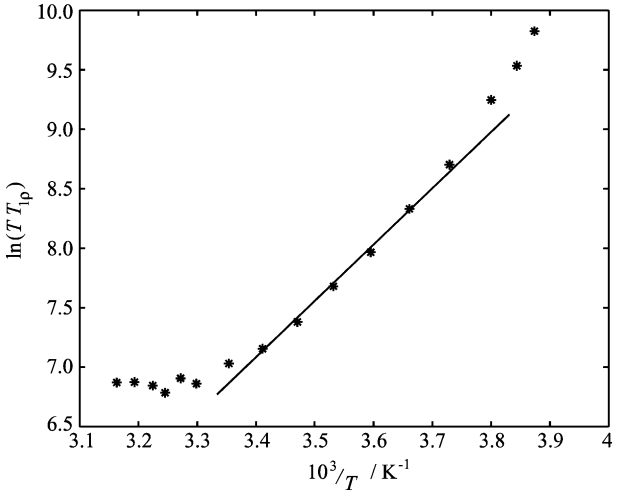

Fig. 3. Plot of $\ln(TT_{1\rho})$ vs. $1/T$ for solid C_6F_{12}. Nine ^{19}F spectra were acquired for each value of $T_{1\rho}$ using a v_{rf} of 38 kHz. The superimposed straight line has the slope calculated from the Eyring equation using a mean value of $\Delta H^{\ddagger} = 39\,\text{kJ mol}^{-1}$ derived from earlier solution-state experiments [5,7,18].

$$k = \frac{k_B T}{h} e^{\Delta S^{\ddagger}/R} e^{-\Delta H^{\ddagger}/RT}. \tag{9}$$

In the slow-exchange regime, $v_{\text{rf}} \gg k$, then $T_{1\rho} \propto k^{-1}$ and so

$$\ln T_{1\rho} = -\ln T + \frac{\Delta H^{\ddagger}}{RT} + C. \tag{10}$$

Hence a plot of $\ln(TT_{1\rho})$ vs. $1/T$ should yield a straight line of gradient $\Delta H^{\ddagger}/R$. The experimental data are consistent with such an analysis, although there are clearly other processes at work (fitting to Arrhenius-type behaviour, i.e., $\ln T_{1\rho}$ vs. $1/T$ gives similar results). The behaviour at high temperatures, close to the sublimation point of 51 °C, departs markedly from that expected in that there is no clear $T_{1\rho}$ minimum. This absence of a results characteristic of $k \gg v_{\text{rf}}$, suggests that additional motions are present in this temperature range. The line on the figure is derived from a mean of solution-state results for the activation energy [5,7,18] and is clearly consistent with the solid-state results. The barriers to exchange in the solid, solution, and gas [18] phases cannot be, therefore, be distinguished within experimental error. This is unsurprising given that localised intermolecular interactions must necessarily be negligible in a molecule forming a plastic crystal phase.

5. Implications for *J*-coupling-based experiments

The ability to resolve J-couplings is crucial to the successful transfer of many solution-state experiments to solid samples. In simple terms, the interference between homonuclear decoupling and motion clearly reduces the "life-time" of the spin states. If the resulting

exchange-induced broadenings exceed the size of the J-couplings, then it will be impossible to use these couplings to build up or transfer coherences.

Fig. 4 puts this in more concrete terms using the attached proton test adapted for solids [2]. After cross-polarisation from the abundant spins (^{19}F in this case), the ^{13}C magnetisation evolves under the influence of the J_{CF} couplings (chemical shift evolution being refocused by the π pulse). As shown in Fig. 4(b), the magnetisation at the end of the τ period oscillates with frequency J_{CF} (scaled by a factor, χ, which depends on the homonuclear decoupling sequence). This oscillation is strongly damped (dashed line) if the conformational exchange rate, k, matches v_{rf} for the homonuclear decoupling. It is also worth noting the apparent frequency of oscillation (and hence any derived J-coupling or scaling factor) is slightly perturbed by the interference. The impact of exchange on the experiment can be conveniently quantified using the magnetisation at $\tau = 1/J_{eff}$. The "refocused fraction," $f = S(1/J_{eff})/S(0)$, will be unity for an undamped oscillation and will tend to zero as the degree of interference between RF irradiation and exchange increases.

The influence of the exchange of the the dynamics of ^{19}F spin system can also be probed directly using the ^{19}F $T_{1\rho}$. Magnetisation is tilted on to the effective spin-lock axis for the homonuclear decoupling sequence involved

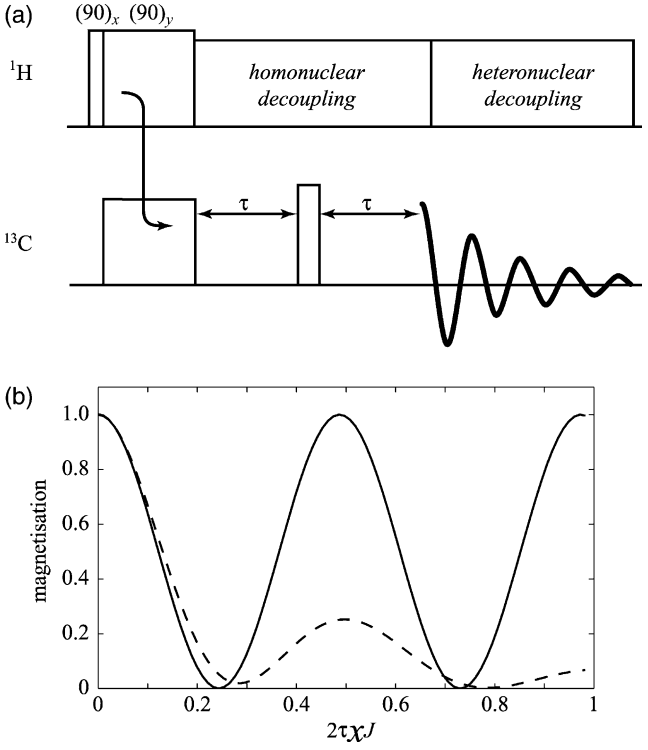

Fig. 4. (a) Pulse sequence for a solid-state version of the attached proton test experiment [2], (b) evolution during BLEW-12 decoupling simulated for a CF_2 unit in the absence of exchange (solid line) and when the exchange rate k equals the RF amplitude, v_{rf} (dashed line).

(at the magic angle in the case of Lee–Goldburg decoupling) and the intensity of the spin-locked magnetisation measured as a function of time. In the absence of exchange broadening, the decay of the spin-locked magnetisation is monoexponential with time constant $T_{1\rho}$. The exchange leads to an additional decay, with time constant T_c.

Fig. 5 plots these two measures, f and the exchange-induced "linewidth" $(1/\pi T_c)$, as a function of exchange rate for three different homonuclear decoupling sequences and two RF field strengths. Unsurprisingly, there is a direct (inverse) between the two measures. The most obvious feature of Fig. 5 is collapse of the polarisation transfer efficiency (solid curve) when the exchange rate matches the RF irradiation frequency; the effectiveness of the polarisation transfer is significantly degraded over about an order of magnitude either side of $k \sim v_{rf}$. The exact position of the interference maximum depends on the decoupling method. For Lee–Goldburg decoupling, for example, this is predicted from Eq. (8) to be at $k = \pi v_{rf}\sqrt{3/2}$. Analytical treatment for other decoupling methods is more difficult, due to the additional time-dependencies, but qualitative predictions can be made. For instance, frequency switched Lee–Goldburg [19] (FSLG) is a more robust method of off-resonance decoupling in which the offset (and phase) are switched after a 2π rotation about the effective field. This modulation introduces an additional frequency component at $v_{eff}/2$, which modestly increases the impact of the interference and shifts the interference maximum to lower exchange rate. This is even more apparent for the BLEW-12 decoupling which cannot be associated with a single timescale; the extent of the interference is significantly worse, both in terms of the range over which the interference occurs and its maximum impact. There may well be advantages to minimise the number and range of frequency components in the effective RF Hamiltonian when designing new homonuclear decoupling sequences [20].

It is interesting to contrast the different effects on the $\{^1H\}^{13}C$ spectrum of physical exchange of the protons compared to flip-flops of the proton spin states due to "spin diffusion." In the absence of proton-decoupling, the spectrum of a CH_2 group under high-speed spinning should tend towards that seen in the solution-state, i.e., a 1:2:1 triplet from the $^1J_{CH}$ couplings. In a study of adamantane at high spinning speeds, Ernst et al. observed instead a *partially* broadened triplet, superimposed on a sharp central peak [15]. The broadening was attributed to the presence of proton spin-flips from "spin diffusion" even at the highest spinning speeds used (30 kHz). This phenomenon could be successfully modelled in terms of Bloch equations modified for exchange. It is important to note that the different mechanisms involved (exchange of spin states due to homonuclear dipolar couplings and physical exchange of spins) give

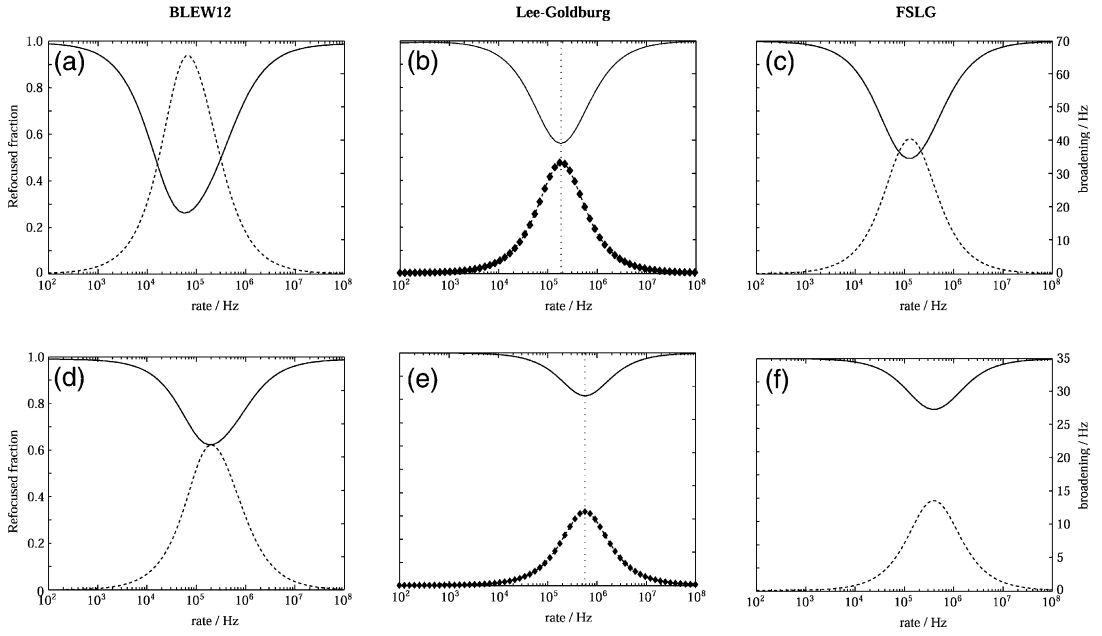

Fig. 5. Plots of ^{13}C magnetisation (solid curve, left-hand scale) at $\tau = 1/J_{\text{eff}}$ as a function of exchange rate for the solid-state APT experiment using two RF field strengths: $\nu_{\text{rf}} = 50$ kHz (a–c) and $\nu_{\text{rf}} = 150$ kHz (d–f), (a, d) BLEW-12 homonuclear decoupling, (b, e) off-resonance irradiation at the magic angle (Lee–Goldburg homonuclear decoupling), (c, f) frequency-switched Lee–Goldburg decoupling. The dashed curves (right-hand scale) show the contribution to the effective ^{19}F linewidth under RF irradiation ($1/\pi T_c$). The black diamonds for the case of off-resonance decoupling show the predictions of Eq. (8). The vertical dotted line marks $k = \pi\nu_{\text{rf}}\sqrt{3/2}$.

rise to different spectral features. In the former case, the spin dynamics of the equivalent protons of the CH_2 group are conveniently described using the coupled representation: a pseudo-spin 0 which does not couple to other spins and a pseudo-spin 1 which is broadened by coupling to other protons [15]. This gives rise to the observed sharp peak superimposed on a broad triplet. Genuine chemical exchange, however, causes complete exchange of the coherences, resulting in broadenings that are described by a single linewidth parameter (this is explored in more detail in Appendix A).

6. Conclusions

The interference between radio-frequency pulse schemes for homonuclear decoupling and chemical exchange has a significant impact on the NMR spectrum of spins coupled to the irradiated spins. The interference becomes greater with increased "complexity" of the RF decoupling, with weaker RF fields and increased chemical shift differences between the exchanging spins (cf. Eq. (8)).

These effects can be readily modelled and provide a useful confirmation of the model used for exchange. Quantitative use of these interference effects is made difficult by the numbers of experimental parameters involved and the correlations between them. Fitting on the ^{19}F spectra would be considerably more robust, but is complicated by the requirement for homonuclear decoupling to remove the ^{19}F–^{19}F intermolecular interactions. The measurement of $T_{1\rho}$ relaxation times provides a more straight-forward route for observing these effects (once the nature of the relaxation process is clear). Measuring $T_{1\rho}$ under Lee–Goldburg conditions assists in isolating different environments by suppressing spin diffusion. More sophisticated techniques of homonuclear decoupling are unlikely to be useful since their use greatly increases the sensitivity to experimental artifacts such as phase transients [21].

The existence of this interference mechanism is also significant for experiments relying on homonuclear decoupling to resolve heteronuclear J-couplings. Although the average Hamiltonian for the spin system under MAS and homonuclear decoupling may only contain effective chemical shifts and J-couplings, this treatment is only valid in the absence of other time-dependencies on a similar timescales. This condition is clearly broken by chemical exchange on the kHz timescale. As a result, the performance of experiments relying on resolved J-couplings will be degraded. Changing the temperature of the sample, and hence the exchange rate, may be sufficient to avoid this interference and will distinguish it from other causes of resolution loss, e.g., interference between sample spinning and RF irradiation [22].

Appendix A. Derivation of exchange line-broadening from Liouville space treatment

It is useful to establish the connection between the simulations of the CF_2 sub-system using the stochastic

Liouville equation, Eq. (4), and the expression for the effect of exchange on $T_{1\rho}$ derived semi-classically [17].

When determining $T_{1\rho}$ for the ^{19}F spins, it is only necessary to consider the simple system of two exchanging ^{19}F spins. Moreover, in C_6F_{12} the dipolar interaction between the spins is eliminated by the rapid motion, while the J-coupling between the spins is negligible. In the absence of couplings between the spins, we only require a composite Liouville space consisting of the direct sum, $\mathscr{L}_1 \oplus \mathscr{L}_2$, of the (4×4) Liouville spaces for the spins, rather than the product space, $\mathscr{L}_1 \otimes \mathscr{L}_2$ [23]. This reduces the size of the Liouvillians from the order 64 (4^3) matrices used above for the simulations of CF_2, to matrices of rank 8 $(4 + 4)$ for the uncoupled F_2 system.

The Liouvillian for the exchanging two-spin system is then

$$\begin{aligned}\hat{L} &= -\mathrm{i}\,\hat{H} + kX \\ &= -\mathrm{i}\begin{pmatrix} \hat{H}_+ & 0 \\ 0 & \hat{H}_- \end{pmatrix} + k\begin{pmatrix} -\mathbf{1} & \mathbf{1} \\ \mathbf{1} & -\mathbf{1} \end{pmatrix},\end{aligned} \tag{A.1}$$

where $\hat{H}_\pm$ is the hamiltonian superoperator for the two spins, which are distinguished by their shifts, $\pm\Delta/2$ (relative to the transmitter). The identity matrices, $\mathbf{1}$, span the 4×4 Liouville space for one spin. The problem is most conveniently expressed in a tilted rotating frame with the z axis along the effective RF field. This axis transformation commutes with X and so the Hamiltonian is:

$$H_\pm = \pm\frac{\Delta \sin\theta}{2} S_x + \left(\pm\frac{\Delta\cos\theta}{2} \pm v_{\mathrm{eff}} \right) S_z. \tag{A.2}$$

In this frame of reference, z-magnetisation will be locked by the strong RF irradiation. In order to distinguish the component of the density matrix proportional to the identity, I (which is not expected to evolve) from z-magnetisation, we write the Liouville space basis: $I \equiv (|\alpha\rangle|\alpha\rangle + |\beta\rangle|\beta\rangle)/\sqrt{2}$, $I_+ \equiv |\alpha\rangle|\beta\rangle$, $I_- \equiv |\beta\rangle|\alpha\rangle$, $I_z \equiv (|\alpha\rangle|\alpha\rangle - |\beta\rangle|\beta\rangle)/\sqrt{2}$.

The Liouvillian is approximately block-diagonalised by taking symmetric and anti-symmetric combinations of the spins, i.e., applying the transformation

$$\hat{L}' = U\hat{L}U', \quad \text{where } U = \frac{1}{\sqrt{2}}\begin{pmatrix} \mathbf{1} & \mathbf{1} \\ \mathbf{1} & -\mathbf{1} \end{pmatrix}. \tag{A.3}$$

Using superscript + and − to label the resulting "sum" and "difference" states, the resulting Liouvillian matrix is then:

$$\begin{array}{c} \\ I^+ \\ I_+^+ \\ I_-^+ \\ I_z^+ \\ I^- \\ I_+^- \\ I_-^- \\ I_z^- \end{array}\!\!\begin{array}{c} \begin{array}{cccccccc} I^+ & I_+^+ & I_-^+ & I_z^+ & I^- & I_+^- & I_-^- & I_z^- \end{array} \\ \begin{pmatrix} 0 & 0 & 0 & 0 & 0 & 0 & 0 & 0 \\ 0 & -\mathrm{i}\ \omega_{\mathrm{rf}} & 0 & 0 & 0 & -\mathrm{i}\pi\Delta c & 0 & \mathrm{i}\pi\Delta s/\sqrt{2} \\ 0 & 0 & \mathrm{i}\ \omega_{\mathrm{rf}} & 0 & 0 & 0 & \mathrm{i}\pi\Delta c & -\mathrm{i}\pi\Delta s\sqrt{2} \\ 0 & 0 & 0 & 0 & 0 & \mathrm{i}\pi\Delta s/\sqrt{2} & -\mathrm{i}\pi\Delta s/\sqrt{2} & 0 \\ 0 & 0 & 0 & 0 & -2k & 0 & 0 & 0 \\ 0 & -\mathrm{i}\pi\Delta c & 0 & \mathrm{i}\pi\Delta s/\sqrt{2} & 0 & -\mathrm{i}\omega_{\mathrm{rf}} - 2k & 0 & 0 \\ 0 & 0 & \mathrm{i}\pi\Delta c & -\mathrm{i}\pi\Delta s/\sqrt{2} & 0 & 0 & \mathrm{i}\ \omega_{\mathrm{rf}} - 2k & 0 \\ 0 & \mathrm{i}\pi\Delta s/\sqrt{2} & -\mathrm{i}\pi\Delta s/\sqrt{2} & 0 & 0 & 0 & 0 & -2k \end{pmatrix} \end{array}, \tag{A.4}$$

where s and c are short-hand for $\sin\theta$ and $\cos\theta$, respectively. I_z^+ corresponds to the sum z-magnetisation which is expected to be locked along the spin-lock axis. This is "lock" is confirmed by the approximately diagonal structure of the Liouvillian; in the limit of $\Delta \ll v_{\mathrm{rf}}$, the off-diagonal elements (which are of the order of Δ) are small compared to the diagonal elements (which involve ω_{rf} and k). The eigenvalue corresponding to the evolution frequency of the I_z^+ state can thus be determined to a good approximation using perturbation theory to second order:

$$E_j = L_{jj} + \sum_{i \neq j} \frac{L_{ij}L_{ji}^*}{L_{ii} - L_{jj}} \tag{A.5}$$

hence

$$\begin{aligned} E(I_z^+) &= \frac{\pi^2\Delta^2\sin^2\theta}{2}\left(\frac{1}{-\mathrm{i}\ \omega_{\mathrm{rf}} - 2k} + \frac{1}{\mathrm{i}\omega_{\mathrm{rf}} - 2k} \right) \\ &= 2\pi^2\Delta^2\sin^2\theta\frac{k}{\omega_{\mathrm{rf}}^2 + 4k^2}. \end{aligned} \tag{A.6}$$

This eigenvalue is purely real, corresponding to an evolution with zero frequency but a non-zero decay constant, $E(I_z^+) = 1/T_{1\rho}$. This result is identical to that obtained using a semi-classical description of exchange, Eq. (8). Extension to multi-pulse decoupling schemes (even ones as closely related as FSLG) is non-trivial, since the propagators for individual pulse sequence elements do not commute. As a result, the eigenvalues of the effective Liouvillian for the complete sequence are not related in any simple way to those of the individual elements. Although it provides less insight, numerical simulation as described earlier is straightforward for these cases. It is interesting to note, however, that the evolution under multi-pulse decoupling techniques is expected to be multi-exponential.

References

[1] K.W. Zilm, D.M. Grant, High-resolution NMR spectra with *J* couplings in solids, J. Magn. Reson. 48 (1982) 524–526.

[2] A. Lesage, S. Steuernagel, L. Emsley, Carbon-13 spectral editing in solid-state NMR using heteronuclear scalar couplings, J. Am. Chem. Soc. 120 (1998) 7095–7100.

[3] D. Sakellariou, L. Emsley, Through-bond experiments in solids, in: D.M. Grant, R.K. Harris (Eds.), Encyclopaedia of Nuclear Magnetic Resonance, vol. 9, Wiley, New York, 2002.

[4] G.V.D. Tiers, Fluorine nuclear spin resonance III. The slow conformation isomerisation of perfluorocyclohexane and the nature of rotational potential barriers in fluorocarbons, Proc. Chem. Soc. (1960) 389–390.

[5] H.S. Gutowsky, F.M. Chen, Spin-echo nuclear magnetic resonance. V. Perfluorocyclohexane, J. Phys. Chem. 69 (1965) 3216–3217.

[6] J.D. Ellet Jr., U. Haeberlen, J.S. Waugh, High resolution nuclear magnetic resonance of solid perfluoro[cyclo]hexane, J. Am. Chem. Soc. 92 (2) (1970) 411–412.

[7] G.V.D. Tiers, Fluorocarbon sulfides: 4. The slow conformational isomerization of perfluorodithianes, J. Fluor. Chem. 90 (1998) 97–100.

[8] J.R. Long, B.Q. Sun, A. Bowen, R.G. Griffin, Molecular dynamics and magic angle spinning NMR, J. Am. Chem. Soc. (1994) 11950–11956.

[9] M. Mehring, Principles of High Resolution NMR in Solids, second ed., Springer, Berlin, 1983.

[10] P. Jackson, R.K. Harris, Proton CRAMPS of NH_3^+ groups: line broadening and molecular dynamics, J. Chem. Soc. Faraday Trans. 91 (5) (1995) 805–809.

[11] J.W. Emsley, L. Phillips, V. Wray, Fluorine Coupling Constants, Pergamon Press, New York, 1977.

[12] D.P. Burum, M. Linder, R.R. Ernst, Low-power multipulse line narrowing in solid-state NMR, J. Magn. Reson. 44 (1981) 173–188.

[13] S.A. Smith, W.E. Palke, J.T. Gerig, Superoperator propagators in simulations of NMR spectra, J. Magn. Reson. Ser. A 106 (1) (1994) 57–64.

[14] P. Hodgkinson, L. Emsley, Numerical simulation of solid-state NMR experiments, Prog. Nucl. Magn. Reson. Spectrosc. 36 (3) (2000) 201–239.

[15] M. Ernst, A. Verhoeven, B.H. Meier, High-speed magic-angle spinning ^{13}C MAS NMR spectra of adamantane: self-decoupling of the heteronuclear scalar interaction and proton spin diffusion, J. Magn. Reson. 130 (1998) 176–185.

[16] W.P. Rothwell, J.S. Waugh, Transverse relaxation of dipolar coupled spin systems under rf irradiation: detecting motions in solids, J. Chem. Phys. 74 (5) (1981) 2721–2732.

[17] H. Desvaux, N. Birlirakis, C. Wary, P. Berthault, Study of slow molecular motions in solution using off-resonance irradiation in homonuclear NMR. II. Fast chemical exchange processes, Mol. Phys. 86 (5) (1995) 1059–1073.

[18] R.J. Morrow, NMR experiments involving population transfer relaxation and chemical exchange, Ph.D. thesis, University of East Anglia, 1982.

[19] M.H. Levitt, A.C. Kolbert, A. Bielecki, D.J. Ruben, High-resolution ^1H NMR in solids with frequency-switched multiple-pulse sequences, Solid State Nucl. Magn. Reson. 2 (1993) 151–163.

[20] D. Sakellariou, A. Lesage, P. Hodgkinson, L. Emsley, Homonuclear dipolar decoupling in solid-state NMR using continuous phase modulation, Chem. Phys. Lett. 319 (3/4) (2000) 253–260.

[21] A. Ramamoorthy, C.H. Wu, S.J. Opella, Experimental aspects of multidimensional solid-state NMR correlation spectroscopy, J. Magn. Reson. 140 (1999) 131–140.

[22] D. Suwelack, W.P. Rothwell, J.S. Waugh, Slow molecular motion detected in the NMR spectra of rotating solids, J. Chem. Phys. 73 (1980) 2559–2569.

[23] R.R. Ernst, G. Bodenhausen, A. Wokaun, Principles of Nuclear Magnetic Resonance in One and Two Dimensions, Clarendon Press, Oxford, 1987.